change of surface emission at 300 K (~6.1 W $m^{-2}$ $K^{-1}$) and are larger than previously derived satellite values (*9*, *12*, *19*, *20*) as shown in Table 1.

During the time of the experiment, differences (up to 40%) in precipitable water and convective activity were observed between regions east and west of the dateline (*19*). Therefore, the data were divided into two groups to produce tropospheric greenhouse effect profiles in convectively suppressed (east) and convectively active (west) regions. The profiles shown in Fig. 4 were constructed by using P-3 data for the mid- and lower troposphere (400 mbar and below), Learjet data for the upper troposphere (~191 mbar), and ER-2 data for the tropopause (~69 mbar). A comparison of the $G_a$ profiles suggests that the greenhouse absorption is greater in the convectively active region west of the dateline at every level measured by the aircrafts. Our sample in the convectively active region is not large enough to prove this point; however, vertical profiles of atmospheric temperature and humidity measured with dropsondes launched from the learjet in conjunction with the radiometric measurements provide further support for this observation. The greenhouse effect was computed from these soundings with a radiative transfer model (*21*, *22*). Regression of the calculated $G_a$ against SST and satellite indices of convective activity also gives values for $G_a$ that are systematically larger in convective regions. The analysis also shows that the perturbations in $G_a$ by convection at fixed SST are comparable in magnitude with the effect of increasing SST by 2 K. This effect results primarily from local moistening of the atmospheric column by deep convection.

Lubin (*23*) finds $dF_a^-/d(\mathrm{SST}) > 4\sigma(\mathrm{SST})^3$ for surface observations, and our results show $dG_a/d(\mathrm{SST}) > 4\sigma(\mathrm{SST})^3$ for tropopause and tropospheric measurements. Furthermore, by comparison we find $dG_a/d(\mathrm{SST}) \approx d(F_a^-)/d(\mathrm{SST})$, demonstrating that the radiation absorbed as greenhouse effect is radiated back to the surface and contributes to surface heating (Fig. 5). The observed net surface heating due to the water vapor greenhouse effect affects those regions of the tropical oceans that have been shown by general circulation model studies to be key areas for climate change and global warming.

## REFERENCES AND NOTES


1. N. E. Graham, *Science* **267**, 666 (1995).
2. P. D. Jones, T. M. Wigley, P. B. Wright, *Nature* **322**, 430 (1986).
3. J. Hansen and S. Lebedeff, *J. Geophys. Res.* **92**, 13345 (1987).
4. J. K. Angell, *Geophys. Res. Lett.* **17**, 1097 (1990).
5. Y. H. Pan and A. H. Oort, *Mon. Weather Rev.* **111**, 1244 (1983).
6. R. E. Newell and B. C. Weare, *Nature* **262**, 40 (1976); *Science* **194**, 1413 (1976).
7. M. Lal and V. Ramanathan, *J. Atmos. Sci.* **41**, 2238 (1984).
8. A. Raval and V. Ramanathan, *Nature* **342**, 758 (1989).
9. G. L. Stephens and T. J. Greenwald, *J. Geophys. Res.* **96**, 15311 (1991).
10. R. Hallberg and A. K. Inamdar, *J. Clim.* **6**, 920 (1992).
11. T. H. VonderHaar, *NASA Refer. Publ.* **1169**, 87 (1986).
12. V. Ramanathan and W. Collins, *Nature* **351**, 27 (1991).
13. F. P. J. Valero, W. J. Y. Gore, L. P. Giver, *Appl. Opt.* **21**, 831 (1982).
14. P. D. Hammer, F. P. J. Valero, S. Kinne, *Mon. Weather Rev.* **119**, 1673 (1991).
15. R. W. Reynolds, *J. Clim.* **1**, 75 (1988).
16. J. D. Spinhirne, W. D. Hart, D. L. Hlavka, *J. Atmos. Sci.* **53**, 1438 (1996).
17. M. D. King *et al.*, *J. Atmos. Oceanogr. Tech.* **13**, 777 (1996).
18. V. Ramanathan *et al.*, *Science* **243**, 57 (1989).
19. Calculations, in which temperature and water vapor profiles obtained with soundings from the research vessel Vickers and climatological summer time profiles above 150 mbar were used, show that the difference between top-of-the-atmosphere and tropopause irradiances is 1.6 W $m^{-2}$ at a fixed 4- to 40-μm bandpass with no change in $dG_a/d(\mathrm{SST})$. The top-of-the atmosphere 4- to 500-μm and 4- to 40-μm irradiances differ by 10 W $m^{-2}$ with no effect in $dG_a/d(\mathrm{SST})$.
20. The satellite data represent a global 5-year record, whereas our data cover 1 month of observations in the central Pacific. We have used the National Center for Atmospheric Research community climate model to check this point. The model reproduces the satellite $dG_a/d(\mathrm{SST})$ very accurately [J. T. Kiehl and B. P. Briegleb, *J. Geophys. Res.* **97**, 10037 (1992)]. However, when the model output is conditionally sampled with the bivariate probability distribution of SST and outgoing longwave radiation corresponding to the domain and time period of our experiment, the model yields $G_a = [147.4 + 13.0(\mathrm{SST} - 300)]$ W $m^{-2}$ at the tropopause. This result is very close to the aircraft values. Because the same model can reproduce both the satellite and aircraft results, depending on how its output is sampled, we conclude that the observed difference may be a consequence of conditions sampled during the observations.
21. C. P. Weaver, W. D. Collins, H. Grassl, *J. Geophys. Res.* **99**, 25891 (1995).
22. The dropsondes released from the Learjet provided reliable data only at pressures higher than 245 mbar. A calculation of $G_a$ at 300 mbar gives $G_a = [134.9 + 13.1(\mathrm{SST} - 300)]$ W $m^{-2}$.
23. D. Lubin, *Science* **265**, 224 (1994).


24. We thank V. Ramanathan for helpful discussions and critical reading of the manuscript. Supported by NSF grant 9223467. The NASA Radiation Sciences Program facilitated the use of the ER-2 aircraft during the experiment.

30 September 1996; accepted 30 January 1997


# Direct Radiative Forcing by Smoke from Biomass Burning


Peter V. Hobbs, Jeffrey S. Reid, Robert A. Kotchenruther, Ronald J. Ferek, Ray Weiss



**Airborne measurements in smoke from biomass burning in Brazil have yielded optical parameters that permit an improved assessment of the effects of smoke on Earth's radiation balance. The global-mean direct radiative forcing due to smoke from biomass burning worldwide is estimated to be no more than about −0.3 watt per square meter (cooling), compared with +2.45 watts per square meter (warming) due to anthropogenic greenhouse gases. On regional scales, direct radiative forcing due to smoke can be large and might indirectly affect global climate.**


Radiative forcing (*1*) due to increases in long-lived greenhouse gases since preindustrial times is know rather precisely: +2.45 ± 0.37 W $m^{-2}$ (*2*). Direct radiative forcing (DRF) due to increases in anthropogenically derived aerosols, on the other hand, is quite uncertain: −0.5 W $m^{-2}$ is the global average, with an uncertainty of at least a factor of 2 (*2*, *3*). Until the magnitude of radiative forcing due to anthropogenically derived aerosols is known more precisely, the uncertainty in the estimate of the net radiative forcing due to anthropogenic emissions of gases and particles, and therefore predictions of global warming, will remain unacceptably large.

The main contributors to radiative forcing by anthropogenic aerosols are believed to be sulfate particles from fossil fuel combustion and smoke particles from biomass burning. About 80% of all biomass burning occurs in the tropics, and South America accounts for about 30% of all tropical burning (*4*). Penner *et al.* (*5*) estimated the global-mean DRF due to biomass burning to be −0.8 W $m^{-2}$ (*6*). We describe here a comprehensive set of measurements of the optical properties of smoke from biomass burning in Brazil (*7*). We then assess the effects of these measurements on estimates of the global-mean DRF due to smoke from biomass burning using a model similar to that used by Penner *et al.*

To quantify DRF due to aerosols, the magnitudes of four optical properties of the aerosols are required: the mass light-scattering efficiency, the fraction of solar radiation backscattered to space, the single-scattering albedo [that is, the ratio of the light-scattering coefficient ($\sigma_s$) to the total extinction


P. V. Hobbs, J. S. Reid, R. A. Kotchenruther, R. J. Ferek, Department of Atmospheric Sciences, University of Washington, Seattle, WA 98195–1640, USA.
R. Weiss, Radiance Research, Seattle, WA 98177, USA.

coefficient], and the effect of relative humidity (RH) on the light scattering. Measurements were obtained on smoke produced by the burning of cerrado, pastures, and primary forests in Brazil in the vicinity of Cuiaba, Porto Velho, and Maraba (Fig. 1), which were chosen to sample regional smoke with different characteristics (8). All of the measurements were made from the University of Washington's research aircraft (9). Light-scattering measurements at wavelengths of 450, 550, and 700 nm were obtained with a nephelometer (*10*), which had a backscatter shutter to determine the total hemispheric backscatter fraction (90° to 170°). Aerosols were sampled continuously through an isokinetic inlet and dried to RH < 30%.

Polytetraethylene (Teflon) filters exposed to the smoke were weighed to determine the dry mass of the smoke. The filters were also analyzed by the integrating plate method (*11*), to determine black carbon content and the integrated aerosol light absorption coefficient ($\sigma_a$), and by ion chromatography. Overall, the measured ionic species together with black carbon accounted for less than 30% of the aerosol dry mass. The remainder of the aerosol mass was largely organics.

The particle mass scattering efficiency $\alpha_s$ is defined by

$$\sigma_s \cong \alpha_s \cdot c_m \cdot f(\mathrm{RH}) \quad (1)$$

where $c_m$ is the mass concentration of the particles and $f$(RH) represents the change in $\sigma_s$ with RH. For a wavelength of 550 nm, we obtained dry mass scattering efficiencies for the smoke ranging from 2.8 to 3.3 $m^2$ $g^{-1}$ (Table 1) (*12*).

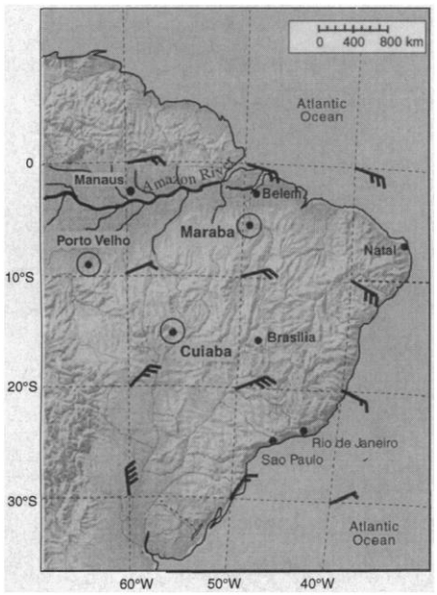


**Fig. 1.** Locations of the three main study areas in Brazil (dots surrounded by circles) and representative winds at 850 mbar for the study period.

On average, the youngest regional smoke was encountered in Maraba, and the oldest smoke, in Porto Velho (Fig. 1). The dry mass scattering efficiency increased with the age of the smoke (Table 1). This increase was attributable to the growth of smoke particles by coagulation and gas-to-particle conversion into a size range where they scattered light more efficiently. The median diameter of smoke increased from 0.12 ± 0.02 μm close to their sources to 0.18 ± 0.06 μm in the regional smoke, and the dry masses of the particles increased from between about 30 and 100% as they aged over several days. The measurements presented in the remainder of this report are for well-aged smoke, which is of most relevance to climate modification.

The nephelometer provided measurements of the fraction of solar radiation that would be scattered backwards by a thin layer of smoke when the sun was directly overhead [β(1)]. This measurement was converted to an average value ($\bar{\beta}$) of solar radiation backscattered during the course of a day by accounting for all possible sun angles (*13*). At a wavelength of 550 nm, $\bar{\beta}$ ranged from 0.24 to 0.26 (Table 1).

The particle mass absorption efficiency $\alpha_a$ is defined by

$$\sigma_a \cong \alpha_a \cdot c_m \quad (2)$$

We derived values of $\alpha_a$ from Eq. 2 using our measurements of $\sigma_a$ and $c_m$ (Table 1). The mass absorption efficiencies for smoke measured in the vicinities of Porto Velho and Maraba (0.64 and 0.62 $m^2$ $g^{-1}$, respectively, at a wavelength of 550 nm) were significantly lower than that for the Cuiaba region (0.83 $m^2$ $g^{-1}$).

If the mass absorption efficiency of black carbon is assumed to be independent of wavelength in the visible spectrum, our measurements of the light absorption coefficient and the wavelength-dependent mass scattering efficiency of smoke can be combined to yield the single-scattering albedo ($\omega_0$) of the smoke (Table 1). At a wavelength of 550 nm, we obtained mean values of $\omega_0$ for dry smoke particles in the range of 0.82 to 0.84. Concurrent measurements of absorption yielded a mean value of 0.84. These values for the single-scattering albedo of smoke in Brazil are lower than those measured by Radke *et al.* (*14*) for boreal fires (0.85 to 0.90), but they are roughly the same as those given by Radke *et al.* (*15*) for smoke from a wide range of fires at mid-latitudes (0.80 to 0.85).

Measurements of $f$(RH) were obtained by drawing smoke samples into a nephelometer and measuring $\sigma_s$ as the smoke

**Table 1.** Optical parameters for dry smoke particles measured in regional hazes at three locations in Brazil. Values given are means and standard deviations.

| Wavelength (nm) | $\alpha_s$ ($m^2$ $g^{-1}$) | β(1) | $\bar{\beta}$ | $\alpha_a$ ($m^2$ $g^{-1}$) | $\omega_0$ |
|---|---|---|---|---|---|
| | | | *Maraba* | | |
| 450 | 3.6 ± 0.75 | 0.11 ± 0.015 | 0.24 ± 0.01 | | 0.86 ± 0.015 |
| 550 | 2.8 ± 0.75 | 0.12 ± 0.015 | 0.25 ± 0.01 | 0.62 ± 0.10 | 0.81 ± 0.020 |
| 700 | 1.6 ± 0.5 | 0.15 ± 0.015 | 0.28 ± 0.01 | | 0.71 ± 0.030 |
| | | | *Porto Velho* | | |
| 450 | 4.2 ± 0.9 | 0.10 ± 0.01 | 0.23 ± 0.01 | | 0.87 ± 0.036 |
| 550 | 3.3 ± 0.75 | 0.11 ± 0.01 | 0.24 ± 0.01 | 0.64 ± 0.13 | 0.84 ± 0.046 |
| 700 | 1.9 ± 0.5 | 0.14 ± 0.015 | 0.27 ± 0.01 | | 0.75 ± 0.065 |
| | | | *Cuiaba* | | |
| 450 | 4.3 ± 1.0 | 0.12 ± 0.02 | 0.25 ± 0.015 | | 0.84 ± 0.052 |
| 550 | 3.3 ± 1.0 | 0.13 ± 0.03 | 0.26 ± 0.02 | 0.83 ± 0.30 | 0.80 ± 0.063 |
| 700 | 1.8 ± 0.5 | 0.16 ± 0.035 | 0.29 ± 0.025 | | 0.69 ± 0.085 |

**Table 2.** Estimates of DRF and the optical parameters from which they are derived. The first four columns give the mean values of the optical parameters for smoke particles at a wavelength of 550 nm measured in regional hazes near Maraba, Porto Velho, and Cuiaba in Brazil. The remaining four columns show global-mean values due to smoke from biomass burning derived from Eqs. 3 through 5, the measured optical parameters, and a global-mean column burden of smoke of $3.7 \times 10^{-3}$ g $m^{-2}$. The corresponding quantities from Penner *et al.* (*5*) are given on the last line.

| Location | $\alpha_s$ ($m^2$ $g^{-1}$) | $\bar{\beta}$ | $\alpha_a$ ($m^2$ $g^{-1}$) | $f$(RH) | $\tau_s$ | $\tau_a$ | $\Delta\alpha_p$ | DRF (W $m^{-2}$) |
|---|---|---|---|---|---|---|---|---|
| Maraba | 2.8 | 0.25 | 0.62 | 1.4 | 0.014 | 0.0023 | $8.4 \times 10^{-4}$ | −0.29 |
| Porto Velho | 3.3 | 0.24 | 0.64 | 1.1 | 0.014 | 0.0024 | $7.3 \times 10^{-4}$ | −0.25 |
| Cuiaba | 3.3 | 0.26 | 0.83 | 1.1 | 0.013 | 0.0031 | $7.2 \times 10^{-4}$ | −0.25 |
| Penner *et al.* (*5*) | 4.7 | 0.30 | 0.7 | 1.7 | 0.030 | 0.0026 | $2.5 \times 10^{-3}$ | −0.8 |

was exposed to various values of RH (*10*) (Fig. 2A). The mean values of $f$(RH) at RH = 80% [assumed by Penner *et al.* (*5*) and others to be an effective average global RH] ranged from 1.1 to 1.4 (Fig. 2B). A humidification factor must be applied to the value we measured for the dry mass scattering efficiency ($\alpha_s$) of the smoke (3.3 $m^2$ $g^{-1}$). A mean value for $f$(RH) at RH = 80% of 1.3 yields values at 550 nm for $\alpha_s$ and $\omega_0$ of 4.3 $m^2$ $g^{-1}$ and 0.88, respectively. From black carbon measurements of young smoke in Brazil, Kaufman *et al.* (*16*) used Mie theory, and other assumptions, to derive a value of 0.90 for $\omega_0$.

The net change in the mean planetary albedo ($\Delta\alpha_p$) produced by a thin aerosol layer is given by (*17*)

$$\Delta\alpha_p = [T_a^2(1 - A_c)][2(1 - R_s)^2\bar{\beta}\tau_s - 4R_s\tau_a] \quad (3)$$

where $T_a$ is the transmissivity of the atmosphere above the aerosol layer, $A_c$ is the cloud fraction, $R_s$ the reflectivity of the underlying surface, $\tau_s$ and $\tau_a$ are the optical depths for light scattering and light absorption

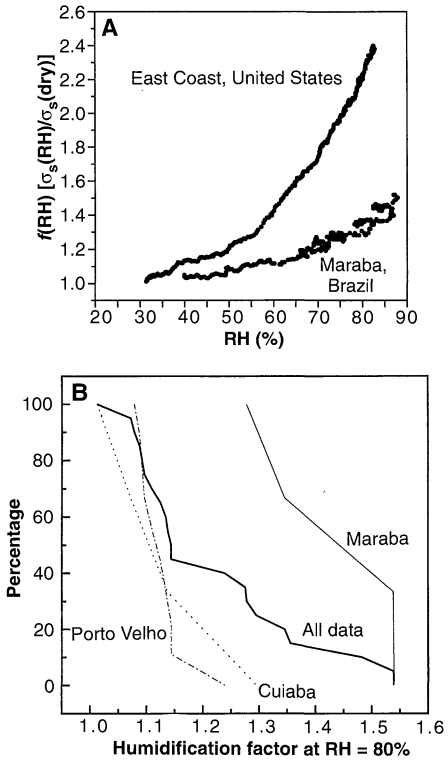


**Fig. 2.** (**A**) A typical plot of $f$(RH) versus RH for smoke in Maraba, Brazil. For comparison, measurements are shown for urban aerosol on the East Coast of the United States. (**B**) Cumulative frequency distribution plot for $f$(RH) of smoke at RH = 80% and a wavelength of 550 nm. The ordinate is the percentage of cases with values of $f$ at RH = 80% that are equal to or greater than the corresponding value on the abscissa.

$$\tau_s = M\alpha_s f(\mathrm{RH}) \quad (4)$$

and

$$\tau_a = M\alpha_a \quad (5)$$

and M is the column burden (in grams per square meter) of the dry aerosol mass. The DRF due to the aerosol layer is given by $\Delta\alpha_p S_0/4$, where $S_0$ is the intensity of solar radiation incident on the aerosol layer.

Penner *et al.* (*5*) used Eqs. 3 through 5 and the best values for the optical constants of smoke available at the time, which derived primarily from measurements of smoke from forest fires in temperate latitudes (*15*), to estimate global-mean values for $\Delta\alpha_p$ and the DRF due to biomass smoke (Table 2). Using the values we measured for the optical constants $\bar{\beta}$, $\alpha_s$, $f$(RH), and $\alpha_a$ of smoke in Brazil and, for the other parameters in Eqs. 3 through 5, the values used by Penner *et al.* [that is, $T_a = 0.76$, $(1 - A_c) = 0.39$, $R_s = 0.15$, and $M = 3.7 \times 10^{-3}$ g $m^{-2}$], we obtain values for $\Delta\alpha_p$, and therefore the global-mean DRF due to smoke from biomass burning, that are about a factor of 3 less than those estimated by Penner *et al.* Thus, our estimate for the global-mean DRF due to aerosols from biomass burning is about $-0.3$ W $m^{-2}$ (Table 2). This value is probably an upper limit for reasons noted in (*6*) and (*13*).

We commonly measured optical depths of 0.4 and sometimes as high as 2.5 over large regions of Brazil, and the column burden of smoke was typically 0.35 g $m^{-2}$. Consequently, on a regional scale in the Amazon Basin, DRF by smoke is substantial. For optical depths greater than about 0.2, a radiative transfer model more sophisticated than that represented by Eqs. 3 through 5 must be used. Also, for a more accurate estimate of the global-mean DRF due to biomass burning and a determination of the uncertainty of this estimate, three-dimensional global model simulations are needed that take into account the geographical distribution and source strengths of the major regions of biomass burning, the dispersion of the smoke over land and ocean, and measurements of the optical properties of the smoke in various regions (*18*).

## REFERENCES AND NOTES


1. Radiative forcing is the perturbation in the energy balance of the Earth-atmosphere system; the sign convention is that positive and negative values indicate warming and cooling, respectively, of the troposphere. For comparison, the net incoming solar radiation at the top of the atmosphere is 342 W $m^{-2}$.
2. J. T. Houghton *et al.*, Eds., *Climate Change 1995: The Science of Climate Change* (Cambridge Univ. Press, Cambridge, 1995); *Climate Change 1994: Radiative Forcing of Climate Change* (Cambridge Univ. Press, Cambridge, 1994) [both published for the Intergovernmental Panel on Climate Change (IPCC)].
3. Not included here is radiative forcing due to the effects of anthropogenic aerosols on clouds (so-called indirect radiative forcing). This effect can also lower temperatures at Earth's surface, but the magnitude of the indirect effect is extremely uncertain. Some recent model calculations [O. Boucher and U. Lohmann, *Tellus B* **47**, 281 (1995)] give a range from $-0.5$ to $-1.5$ W $m^{-2}$ for the globally averaged indirect forcing by anthropogenic sulfate aerosol. The IPCC (*2*), on the other hand, gives a range of 0 to $-1.5$ W $m^{-2}$ for the indirect forcing by all anthropogenic aerosol.
4. W. M. Hao and M.-H. Liu, *Global Biogeochem. Cycles* **8,** 495 (1994).
5. J. E. Penner, R. E. Dickinson, C. A. O'Neill, *Science* **256**, 1432 (1992).
6. The IPCC (*2*) reduced Penner *et al.*'s (*5*) estimate of the global-mean DRF due to smoke from biomass burning by a (rather arbitrary) factor of 4. A factor of 2 was attributed to the use of a simple box model calculation instead of a three-dimensional model, and another factor of 2 was asserted because the period of reference was taken to start at 1850 instead of 1750, because significant changes in biomass burning are thought to have occurred before 1850. Therefore, the IPCC best estimate for the global-mean DRF due to biomass burning since preindustrial times is $-0.2$ W $m^{-2}$. Here we are concerned with a quite different correction to Penner *et al.*'s estimate, namely, that resulting from the use of our measurements of the optical parameters of smoke.
7. Measurements of the optical properties of an aerosol should be made on the same sample, as was done in our study, because there is substantial interdependence and compensation among the various optical properties [O. Boucher and T. L. Anderson, *J. Geophys. Res.* **100,** 26117 (1995)].
8. Our measurements were obtained as part of the Smoke, Clouds, and Radiation–Brazil (SCAR-B) Project in August through September 1995, during a long dry period with considerable biomass burning in Brazil.
9. The instrumentation aboard this aircraft is described by P. V. Hobbs *et al.* [*J. Geophys. Res.* **96**, 18735 (1991)].
10. D. A. Hegg, D. S. Covert, M. J. Rood, P. V. Hobbs, *ibid.* **101**, 12893 (1996).
11. C. Lin, M. Baker, R. Charlson, *Appl. Opt.* **12**, 1356 (1973).
12. In this report "particles" or "smoke" refer to regional hazes dominated by smoke particles. At least 80 to 90% of the mass of the particles in such hazes derived directly from biomass burning. There have been no previous direct measurements of dry mass scattering efficiencies for smoke from tropical biomass burning. Approximate values can be calculated from measured particle size distributions [for example, P. Artaxo *et al.*, *J. Geophys. Res.* **99**, 22857 (1994)], but this method requires assumptions about the shapes and compositions of the particles.
13. J. Hansen, *J. Atmos. Sci.* **26**, 478 (1969); W. J. Wiscombe and G. W. Grams, *ibid.* **33**, 2440 (1976). Y. J. Kaufman and B. N. Holben [*J. Geophys. Res.* **101,** 19433 (1996)] suggest that averaging equally over all solar zenith angles overestimates backscattering from biomass burning aerosol in the tropics by 25%, but we have not included this reduction here.
14. L. F. Radke *et al.*, in *Aerosols and Climate*, P. V. Hobbs and M. P. McCormick, Eds. (Deepak, Hampton, VA, 1988).
15. L. F. Radke *et al.*, in *Global Biomass Burning: Atmospheric, Climatic and Biospheric Implications*, J. S. Levine, Ed. (MIT Press, Cambridge, MA, 1991).
16. Y. J. Kaufman *et al.*, *J. Geophys. Res.* **97**, 14581 (1992).
17. P. Chylek and J. Wong, *Geophys. Res. Lett.* **22**, 929 (1995).
18. Our measurements are for one tropical region (Brazil) during one burning season. There may be annual and geographic differences in the optical properties of smoke.


19. This work was supported by NASA grants NAGW-3750 and NAG 11709; NSF grants ATM-9400760, ATM-9412082, and ATM-9408941; U.S. Environmental Protection Agency grant CR822077; and NOAA grant NA67RJ0155 (PMEL contribution 425).

26 November 1996; accepted 28 January 1997